HHS Public Access

Author manuscript

*Biochem Pharmacol*. Author manuscript; available in PMC 2024 September 01.

Published in final edited form as:

*Biochem Pharmacol*. 2023 September ; 215: 115702. doi:10.1016/j.bcp.2023.115702.

# The regulation of human organic anion transporter 4 by insulin-like growth factor 1 and protein kinase B signaling

**Zhou Yu**,

**Haoxun Wang**,

**Guofeng You***

Department of Pharmaceutics, Rutgers, The State University of New Jersey, 160 Frelinghuysen Road, Piscataway, New Jersey, 08854, USA

## Abstract

Human organic anion transporter 4 (hOAT4), mainly expressed in the kidney and placenta, is essential for the disposition of numerous drugs, toxins, and endogenous substances. Insulin-like growth factor 1 (IGF-1) is a hormone generated in the liver and plays important roles in systemic growth, development, and metabolism. In the current study, we explored the regulatory effects of IGF-1 and downstream signaling on the transport activity, protein expression, and SUMOylation of hOAT4. We showed that IGF-1 significantly increased the transport activity, expression, and maximal transport velocity $V_{max}$ of hOAT4 in kidney-derived cells. This stimulatory effect of IGF-1 on hOAT4 activity was also confirmed in cells derived from the human placenta. The increased activity and expression were correlated well with the reduced degradation rate of hOAT4 at the cell surface. Furthermore, IGF-1 significantly increased hOAT4 SUMOylation, and protein kinase B (PKB)-specific inhibitors blocked the IGF-1-induced regulations on hOAT4. In conclusion, our study demonstrates that the hepatic hormone IGF-1 regulates hOAT4 expressed in the kidney and placenta through the PKB signaling pathway. Our results support the remote sensing and signaling theory, where OATs play a central role in the remote communications among distal tissues.

### Keywords

drug transporter; human organic anion transporter 4; regulation; IGF-1; protein kinase B; SUMOylation

*Corresponding author: Guofeng You, Department of Pharmaceutics, Rutgers, The State University of New Jersey, 160 Frelinghuysen Road, Piscataway, NJ 08854, USA Tel: 848-445-6349; gyou@pharmacy.rutgers.edu.

Author contributions

Zhou Yu: Conceptualization, Data curation, Formal analysis, Visualization, Writing - original draft. Haoxun Wang: Conceptualization; Data curation; Formal analysis. Guofeng You: Funding acquisition; Project administration; Supervision, Writing - original draft.



Declaration of Competing Interest

The authors declare that they have no known competing financial interests or personal relationships that could have appeared to influence the work reported in this paper.

## 1. Introduction

Human organic anion transporter 4 (hOAT4) is a member of the organic anion transporter family (OATs), essential for the disposition of various clinical therapeutics and endogenous substances, such as antibiotics, antiviral drugs, anti-cancer therapeutics, metabolites, and environmental toxins (1–3). hOAT4 is mainly expressed at the proximal tubule cells in the kidney and the syncytiotrophoblasts in the placenta. In the kidney, hOAT4 is primarily involved in the renal reabsorption and excretion of endogenous substances and xenobiotics (e.g., drugs and environmental toxins) (4–6). In the placenta, hOAT4 is mainly responsible for fetal protection and detoxification by removing toxic molecules from the fetus (7,8). Given such importance in physiology and pharmacology, investigating the regulation of hOAT4 has profound clinical significance.

The transport activity of OATs is determined by their protein expression level at the cell surface. Our previous studies have revealed that OATs expressed on the cell membrane are constitutively internalized from and recycled back to the cell membrane, controlling their cell surface expression (3,9–11). The activity and expression of OATs are often regulated by post-translational modifications (PTMs), which alter OAT trafficking and stability through covalent modifications on specific amino acid residues of OATs (3,9–11). The modification by Small Ubiquitin-like Modifier (SUMO) has been discovered as a critical PTM, regulating the trafficking and stability of proteins on plasma membrane and in cell nucleus (12–15). The SUMOylation process is carried out in a three-step mechanism requiring available SUMO molecules and the collective actions of SUMO activating enzymes (E1), SUMO conjugating enzymes (E2), and SUMO ligating enzymes (E3) (12,13). As for the individual SUMO molecules, there are four members (SUMO1/2/3/4) of the SUMO family discovered in mammalian cells. SUMO2 and SUMO3 are 97% identical in protein sequences but they only share 46% identity with SUMO1. The precursor of SUMO4 cannot produce a mature SUMO protein available for SUMO conjugation (12,13). SUMO modification occurs when SUMO molecules (single or multiple) are covalently conjugated to lysine residue(s) of a target protein. Both SUMO2 and SUMO3 can form poly-SUMO chains since they have internal lysine residues matching the consensus motif for SUMOylation. SUMO1, without such lysine residues, is not able to form poly-SUMO chains (12,13,16). Our previous studies have discovered that hOAT3, another member of the OAT family, is a substrate for SUMO modification (17,18). However, whether hOAT4 is a target for SUMO modification and what factors potentially modulate this process have not been investigated.

Recent publications have introduced a hypothesis called Remote Sensing and Signaling. This theory suggests a network of remote communications to maintain homeostasis. And membrane transporters play a central role in this network of communications. These communications between organs are usually carried out by metabolites, hormones, and cell signaling pathways (19,20). For instance, hormones are often synthesized in one organ and released into the blood to regulate transporters in distal tissues through specific cell signaling pathways. Insulin-like growth factor 1 (IGF-1) is such a hormone produced by the hepatocytes in the liver, secreted into the circulation, and arrives at distal tissues to exert its physiological functions (21,22).

Changes in IGF-1 level in the body would lead to several diseases, including Laron syndrome (deficiency in IGF-1 secretion) and Acromegaly (excessive secretion of IGF-1) (23). IGF-1 also plays important roles in renal development and maintaining renal functions. Abnormal IGF-1 signaling would lead to multiple kidney diseases, including acute kidney failure and kidney cancer (21,22,24). At the molecular level, IGF-1 exerts its functions through binding to the IGF-1 receptor at the cell surface. Upon binding, the intracellular domains of IGF-1 receptor auto-phosphorylate and activate downstream signaling proteins (25). IGF-1 regulates target proteins through downstream signaling proteins such as Ras-mitogen-activated protein kinase and protein kinase B (PKB) (21,25,26). PKB, also known as Akt, is a serine/threonine-specific protein kinase which regulates many cell functions such as transcription, cell cycle, metabolism, and apoptosis (27). By phosphorylating its substrates, PKB regulates the activity, expression, and localization of substrate proteins, including glycogen synthase kinase 3β (cell metabolism) and Bcl2-associated agonist of cell death (cell apoptosis) (25,27). However, whether hOAT4 can be regulated by IGF-1 or PKB signaling has never been studied.

In the current study, we investigated the effects and potential mechanism of the regulation of hOAT4 by IGF-1. Our data elucidated the connections between IGF-1 and the transport activity, protein expression, and SUMOylation of hOAT4.

## 2. Materials and methods

### 2.1. Materials

Parental COS-7 cells were purchased from ATCC (Manassas, VA). Parental BeWo cells were generously provided by Dr. Erik Rytting from University of Texas Medical Branch (Galveston, TX). [$^3$H]-labeled estrone sulfate (ES) was purchased from PerkinElmer (Waltham, MA). Membrane-impermeable biotinylation reagent Sulfo-NHS-SS-biotin, streptavidin agarose beads, protein G agarose beads, protease inhibitor cocktail, anti-mouse secondary antibody (7076), and anti-rabbit secondary antibody (7074) were purchased from Cell Signaling Technology (Danvers, MA). Plasmids for HA-tagged SUMO1, SUMO2, and SUMO3 were kindly provided by Dr. Jorge A Iñiguez-Lluhí from the University of Michigan Medical School (Ann Arbor, MI). Mouse anti-myc antibody (11667203001) was obtained from Roche (Indianapolis, IN). Anti-HA (ab9110), anti-SUMO1 (ab32058), anti-SUMO2/3 (ab3742), anti-E-cadherin (ab76055) antibodies were obtained from Abcam (Waltham, MA). Anti-GAPDH antibody (sc47724) was obtained from Santa Cruz Biotechnology (Dallas, TX). 10-DEBC and ipatasertib were purchased from Selleck Chemicals (Houston, TX). IGF-1 was purchased from Sigma-Aldrich (St. Louis, MO). The antibotic G418 was obtained from Invitrogen (Carlsbad, CA). Phosphate-buffered saline, Tween-20, $CaCl_2$, and $MgCl_2$ were purchased from Life technologies (Carlsbad, CA).

### 2.2. Cell Culture and Transfection

Parental COS-7 cells were cultured in DMEM medium from Invitrogen (Carlsbad, CA) containing 10% fetal bovine serum purchased from ThermoFisher Scientific (Waltham, MA) at 37°C in 5% $CO_2$. Cells stably expressing human OAT4 (hOAT4) were previously

generated by our lab (5) and maintained in DMEM medium containing 0.5 mg/mL G418 (Invitrogen, Carlsbad, CA) and 10% fetal bovine serum. Parental BeWo cells were grown in Dulbecco's modified Eagle's/F-12K medium obtained from ATCC (Manassas, VA) supplemented with 10% fetal bovine serum at 37°C in 5% $CO_2$. Transfection with cDNA plasmids was done using Lipofectamine 3000 reagent (Invitrogen, Carlsbad, CA) following the manufacturer's standard protocol. After transfection the cells were incubated for 48 h before following experiments.

### 2.3. Transport Activity Measurement (uptake assay)

In brief, parental or cells stably expressing hOAT4 were plated in 48-well cell culture plates one day before uptake assay. In cells transiently transfected with the plasmids, uptake was performed 48 h after transfection. After removing treatment media, 120 μL of the uptake solution consisting of phosphate-buffered saline (PBS) (pH 7.5) with 1 mM $CaCl_2$, 1 mM $MgCl_2$, and [$^3$H]-estrone sulfate (ES) (0.3 μM) was added to each well to start the 4-min uptake assay at room temperature with gentle shaking. The uptake process was terminated by aspirating the uptake solution and rapidly washing the cells twice with 500 μL of ice-cold PBS. The cells were then lysed with 200 μL of 0.2 N NaOH for 30 min with shaking, neutralized with 200 μL of 0.2 N HCl. The lysates were subjected to liquid scintillation counting (1-min per sample) by a multi-purpose scintillation counter (Beckman LS6500). Transport activity was expressed as a percentage of the uptake values measured in control cells. Uptake data were adjusted for uptake values measured in mock cells (parental COS-7 cells transfected with empty plasmid).

### 2.4. Biotinylation assay

The measurement of cell surface hOAT4 was conducted by using a biotinylation strategy. In brief, cells were seeded in 35-mm cell culture petri dishes. Sulfo-NHS-SS-biotin (0.5 mg/ml in PBS with 1mM $CaCl_2$ and 1mM $MgCl_2$, pH 8.0) was added to each dish to label surface proteins. After biotinylation labeling, the unreacted sulfo-NHS-SS-biotin was quenched by rinsing the cells with 100 mM glycine in PBS (pH 8.0). The cells were then lysed on ice for 45 min. After 15 min centrifugation at 15000 xg at 4 °C, supernatants of cell lysates were added to 40 μL of pre-washed streptavidin-agarose beads to purify the labeled cell membrane proteins. Cell surface hOAT4 (tagged with myc epitope) was detected in the pool of surface proteins by SDS-PAGE and immunoblotting using anti-myc antibody. E-cadherin was also examined as a cell surface protein marker. Total hOAT4 in the cell lysates was directly detected by SDS-PAGE and immunoblotting using anti-myc antibody. GAPDH was measured as a total cellular protein marker.

### 2.5. Degradation assay

The degradation assay of hOAT4 was carried out following the procedure established in our lab (17). In brief, hOAT4-expressing COS-7 cells were subjected to biotinylation labeling with 0.5 mg/ml sulfo-NHS-SS-biotin in PBS at 4 °C. The biotinylation was followed by quenching of the unreacted NHS-SS-biotin with PBS containing 100 mM glycine at 4 °C. The biotin-labeled cells were then incubated in DMEM medium containing IGF-1 at 37°C in a cell culture incubator. Those cells were collected at indicated time points and lysed and centrifuged at 15,000 ×g at 4 °C for 15 min. The supernatants were incubated with 40 μL

of pre-washed streptavidin agarose beads to isolate biotinylated proteins, and cell surface hOAT4 survived from degradation was detected by SDS-PAGE and immunoblotting using anti-myc antibody.

### 2.6. Immunoprecipitation

In brief, cells were lysed with cell lysis buffer (10 mM Tris-HCl, 150 mM NaCl, 1 mM EDTA, 0.1% SDS, 1% Triton X-100, 1% protease inhibitor cocktail) and the same amount of total proteins (800–1000 μg) were incubated with 30 μL of protein G-agarose beads at 4°C for 4 h to reduce non-specific binding. Meanwhile, appropriate primary antibody was incubated with 30 μL protein G-agarose beads at 4°C for 4 h to form antibody-beads complex. The pre-cleared protein samples were then mixed with antibody-bound protein G-agarose beads at 4°C overnight with end-over-end rotating. On the next day, the immunoprecipitated proteins on beads were washed three times and denatured with 2x Laemmli buffer (ThermoFisher Scientific, Waltham, MA), and analyzed by immunoblotting with antibodies indicated in each experiment.

### 2.7. SDS-PAGE and Immunoblotting

We followed the standard procedures provided by Bio-Rad (Hercules, CA). In brief, protein samples were separated on SDS-PAGE minigels (Bio-Rad, Hercules, CA) and electroblotted onto PVDF membranes. The blots were incubated with 5% nonfat dry milk for 2 h in PBST buffer (0.1% Tween-20 in PBS) at room temperature, followed by incubation overnight at 4°C with indicated primary antibodies. Then the blots were washed and incubated with horseradish peroxidase-conjugated secondary antibodies for 4 h at room temperature, followed by detection with SuperSignal West Dura Extended Duration Substrate kit from Thermo Fisher Scientific (Waltham, MA). ChemiDoc imaging system (Bio-Rad, Hercules, CA) was used to capture the non-saturating, immunoreactive bands of target proteins. Imaging Lab software (Bio-Rad, Hercules, CA) was used to quantify target protein bands.

### 2.8. Data Analysis

Each experiment was repeated independently for a minimum of three times and multiple repeats were used for statistical analysis. Between two groups, statistical analysis was performed using Student's paired *t*-tests. Among multiple groups, one-way ANOVA with Post Hoc Tukey's test was applied using GraphPad Prism software (GraphPad Software, San Diego, CA). A $*P$ value of $< 0.05$ was considered statistically significant.

## 3. Results

### 3.1. Effect of IGF-1 on hOAT4 transport activity

To study the effect of IGF-1 on hOAT4 transport activity, COS-7 cells stably expressing hOAT4 were treated with IGF-1 under various doses (1 – 100 nM) and periods of time (1 – 4 h), followed by the quantification of hOAT4-mediated [$^3$H]-estrone sulfate (ES) uptake. ES was widely used as a prototypical substrate for measuring hOAT4 transport activity. As shown in Figure 1a and 1b, IGF-1 significantly stimulated hOAT4 transport activity in a dose- and time-dependent manner.

### 3.2. Effect of IGF-1 on hOAT4 transport kinetics

To explore the mechanism behind the IGF-1-stimulated hOAT4 transport activity, hOAT4-mediated transport of [$^3$H]-ES was measured with a range of substrate concentrations after IGF-1 treatment (100 nM, 2 h). Based on the Eadie-Hofstee plot derived from Michaelis–Menten equation of enzyme kinetics (Figure 2), IGF-1 treatment effectively increased the maximal transport velocity $V_{max}$ of hOAT4-mediated ES uptake (from 92.85 pmol/mg*4min for control group to 116.36 pmol/mg*4min for IGF-1 group), while the substrate-binding affinity ($K_m$) between hOAT4 and ES was not significantly changed (shown as the slopes of the trend lines).

### 3.3. PKB inhibitors blocked IGF-1-induced stimulation of hOAT4 transport activity

IGF-1 has been reported to regulate target proteins through multiple signaling pathways including the PKB pathway (25,27). Therefore, we utilized a PKB-specific inhibitor 10-DEBC to explore the involvement of PKB pathway. As shown in Figure 3a, 7 μM of 10-DEBC completely blocked the stimulatory effect of IGF-1 on hOAT4 transport activity. And 10-DEBC did not show much cytotoxicity effect when used alone at the same concentration. During the past decade, the PKB signaling pathway has drawn much attention in the field of oncology as a novel therapeutic target for multiple types of cancer. Several drug candidates targeting PKB have already entered clinical development (28,29). Therefore, we explored the effect of ipatasertib, a drug under clinical trials for solid tumors and specifically inhibiting PKB, on the hOAT4 transport activity regulated by IGF-1. As shown in Figure 3b, 10 μM of ipatasertib (Ipa) blocked the IGF-1-induced increase of hOAT4 transport activity, and ipatasertib alone didn't show any non-specific cytotoxicity under the same condition. Our results suggest that PKB signaling plays an essential role in the regulation of hOAT4 transport function by IGF-1.

### 3.4. Effects of IGF-1 and ipatasertib on hOAT4 protein expression

The increase of the maximal transport velocity ($V_{max}$) we observed in Figure 2 could be due to either an increase of the amount of hOAT4 at the cell surface or an increased transporter turnover rate. Therefore, we utilized a biotinylation method to determine the underlying cause for the increased transport activity induced by IGF-1. After IGF-1 treatment (100 nM, 2 h) in the absence or presence of ipatasertib (10 μM), we measured hOAT4 protein expression both at the cell surface and in total cell lysates. Our results showed that treatment with IGF-1 increased the expression of hOAT4 both at the cell membrane (Figure 4a, top panel and Figure 4b) and in total cell lysates (Figure 4c, top panel and Figure 4d), while ipatasertib (Ipa) reversed the increasing effects back to control level. Such changes in hOAT4 expression were not due to unequal protein loadings since the expression of cell surface protein marker E-cadherin and total cellular protein marker GAPDH were similar among all groups (Figure 4a, bottom panel and Figure 4c, bottom panel).

### 3.5. Effect of IGF-1 on hOAT4 protein stability

Previously our lab has discovered that protein trafficking and degradation significantly affect the cell surface and total expression of OATs (3,9,30,31). Thus, we further explored whether IGF-1 could affect the degradation rate of cell surface hOAT4, which would directly

contribute to the increased amount of hOAT4 at the cell surface. hOAT4-expressing cells were labelled with membrane impermeable biotinylation reagent, followed by incubation with or without IGF-1 (100 nM) for 2 h and 6 h. The biotin-labeled membrane proteins were subject to immunoblotting (IB) with anti-myc antibody to detect the non-degraded cell surface hOAT4. Our results showed that the degradation rate of hOAT4 was significantly lower after both 2 h and 6 h treatment of IGF-1 when compared to the control group (Figure 5a, top panel and Figure 5b). And at each indicated time points, the cell membrane protein marker E-cadherin showed comparable expression between the control and IGF-1-treated groups (Figure 5a, bottom panel), suggesting the differences in hOAT4 expression were not due to the alteration of overall cell surface proteins. Together, these results indicated that IGF-1 reduces the degradation rate of hOAT4, which leads to an increased amount of the transporter at the cell surface.

### 3.6. Effects of IGF-1 and ipatasertib on hOAT4 SUMOylation

Previously our lab discovered that hOAT3, another important member of the OAT family, is a substrate for SUMOylation modification and the increasing in hOAT3 SUMOylation is correlated with its increased transport activity (17,18). Therefore, we further explored if hOAT4 is a target for SUMO modification and whether IGF-1 can regulate SUMOylation of the transporter. Due to the heterogeneity of SUMO1, SUMO2, SUMO3 in their sequences and roles in SUMOylation, we first investigated whether IGF-1 affects hOAT4 SUMOylation and if so, which of the SUMO isoforms are involved in this process. After IGF-1 treatment (100 nM, 2 h), hOAT4 was immunoprecipitated (IP) and anti-SUMO1 or anti-SUMO2/3 antibodies (IB) were used to detect endogenously SUMOylated hOAT4. The data showed that hOAT4 was indeed modified by endogenous SUMO1/2/3 and IGF-1 only increased the amount of hOAT4 modified by endogenous SUMO2 and SUMO3 (Figure 6b, top panel and 6c). The level of hOAT4 conjugated to SUMO1 remained unchanged after IGF-1 treatment (Figure 6a, top panel and 6c). Similar amount of hOAT4 were pulled down among all groups (Figure 6a, bottom panel and Figure 6b, bottom panel), suggesting the differences in SUMOylated hOAT4 were not caused by unequal amount of hOAT4 pulled down. Since SUMO2 and 3 are small proteins with a molecular weight of ~18 kDa and SUMO1 is about 12 kDa, the attachment of multiple SUMO molecules (individually to different sites or as a poly-SUMO chain) could significantly increase the molecular weight of SUMOylated hOAT4 detected in immunoblots as shown in these results.

Next, since immunoblotting could not distinguish between endogenous SUMO2 and SUMO3 due to their high homology, HA-tagged HA-SUMO2 or HA-SUMO3 were individually transfected into hOAT4-expressing cells. After IGF-1 treatment (100 nM, 2 h), hOAT4 was immunoprecipitated (IP) and anti-HA antibody (IB) was used to detect SUMOylated hOAT4. Our results showed that IGF-1 significantly increased the amount of hOAT4 modified by SUMO2 and SUMO3, though HA-SUMO2 modification displayed a higher degree of increase (Figure 7a, top panel and Figure 7b). Similar quantities of hOAT4 were pulled down among all samples (Figure 6a, bottom panel), suggesting the differences in SUMOylated hOAT4 were not caused by unequal amount of total hOAT4 pulled down. These results indicated that IGF-1 specifically regulates the amount of hOAT4 SUMOylated by both SUMO2 and SUMO3.

Furthermore, we investigated the involvement of PKB pathway in the regulation of hOAT4 SUMOylation. HA-SUMO2 was transfected into hOAT4-expressing cells. After IGF-1 treatment, hOAT4 was immunoprecipitated and anti-HA antibody was utilized to detect SUMOylated hOAT4. As shown in the top panel of Figure 8a and Figure 8b, IGF-1 significantly increased the amount of SUMOylated hOAT4, and this stimulatory effect was abrogated by ipatasertib (Ipa), an anticancer drug and PKB-specific inhibitor. The changes of hOAT4 SUMOylation were not due to the variation in the amount of total hOAT4 since similar quantities of hOAT4 were pulled down among all samples (Figure 8a, bottom panel). These results suggested that IGF-1 up-regulates hOAT4 SUMOylation through PKB signaling.

### 3.7. Effects of IGF-1 and ipatasertib on hOAT4 transport activity in placental BeWo cells

hOAT4 is known to be mainly expressed in the kidney and placenta. Since all our findings above were from kidney-derived cells, in this experiment, we explored the effect of IGF-1 on hOAT4 expressed in BeWo cells derived from human placenta. As shown in Figure 9, the stimulatory effect of IGF-1 on hOAT4 transport activity in BeWo cells was comparable to that in renal COS-7 cells. Again, ipatasertib (Ipa) blocked this stimulatory effect by IGF-1 on hOAT4 while itself did not show non-specific cytotoxicity. Our results indicated that *in vivo* IGF-1 may be capable of regulating hOAT4 expressed in both kidney and placenta.

## 4. Discussion

Human organic anion transporter 4 (hOAT4) is a member of the OAT family, mainly localized in the kidney and the placenta (1–3,32). In the kidney, hOAT4 is localized to the proximal tubule cells and plays important roles in the reabsorption and elimination of many drugs and endogenous metabolites (4–6). In the placenta, hOAT4 is expressed at the syncytiotrophoblasts and is responsible for removing endogenous substances and xenobiotics from the fetus (7,8). Therefore, investigating the regulatory mechanisms of hOAT4 at molecular and cellular levels is of great clinical importance. The current study explored the regulatory effects of insulin-like growth factor 1 (IGF-1) on hOAT4 and the potential mechanism behind this regulation. Our data demonstrated that IGF-1 modulates the transport activity, expression, and SUMOylation of hOAT4 through protein kinase B (PKB) signaling.

Since hOAT4 is primarily expressed in the kidney and the placenta, we conducted our study in kidney-originated COS-7 cells and placenta-originated BeWo cells. Both are considered suitable and reliable systems for studying the activity, expression, and regulation of membrane transporters (2,33–36). Our results showed that IGF-1 stimulated hOAT4-mediated uptake of [$^3$H]-ES in a dose- and time-dependent manner in COS-7 cells (Figure 1) and BeWo cells (Figure 9). These findings in cultured cells will pave the way for further understanding the regulation of hOAT4 *in vivo*. The IGF-1 concentrations at the nM range used throughout this study are consistent with those described in other publications investigating IGF-1 functions (26,36,37). In humans, the serum level of IGF-1 usually reaches maximum during adolescence to facilitate whole-body growth and keeps decreasing during adulthood (21). In a clinical study, the median level of IGF-1 in the serum of healthy

adults is about 380 ng/mL (50 nM) at the age of 18 and 180 ng/mL (24 nM) at the age of 70 (38). Thus, the IGF-1 concentrations used throughout our study are physiologically relevant.

Next, the transport kinetics behind this stimulatory effect from IGF-1 on hOAT4 activity was investigated. The uptake data and corresponding dot plot (Figure 2) demonstrated that IGF-1 increased the maximal transport velocity $V_{max}$ of hOAT4 without changing its substrate-binding affinity $K_m$. Higher amount of hOAT4 expressed at cell surface or an increased turnover rate of the substrate transport can both contribute to the increased $V_{max}$ of hOAT4 transport. Therefore, we examined the effect of IGF-1 on hOAT4 protein expression. The cell surface and total expression of hOAT4 were elevated after IGF-1 treatment (Figure 4), which correlated well with the enhanced transport activity and $V_{max}$ observed. Furthermore, we also revealed that the rate of hOAT4 degradation was significantly slowed after IGF-1 treatment (Figure 5), contributing to the higher amount of hOAT4 at the cell surface and in total lysates.

PKB signaling has been established as one important signaling pathway downstream of IGF-1 (25). In this study, we utilized PKB inhibitors 10-DEBC and ipatasertib to examine the involvement of this pathway in the regulation of hOAT4. Our data showed that the IGF-1-induced increases in hOAT4 activity and expression were abrogated by 10-DEBC and ipatasertib (Figures 3 & 4), suggesting PKB specificity of this regulation by IGF-1. Compared to the classic PKB inhibitor 10-DEBC, ipatasertib is developed as a potent anti-cancer drug that is highly selective for PKB. It has been reported to inhibit the growth of cancer cells and prevent tumor growth in xenograft models (39). It is currently under phase 2 clinical trials for treating solid tumors, including prostate and breast cancer (40,41). Based on *in vitro* kinase inhibition study, ipatasertib exhibits $IC_{50}$ of 5–18 nM for isoforms of PKB (28). According to pharmacokinetic data from a clinical study, the $C_{max}$ of ipatasertib in the serum was about 1000 ng/mL, which was equal to 2.2 μM (40). Therefore, the ipatasertib concentration at the μM range used in our study is pharmacologically relevant. Our work is the first to investigate the interactions between ipatasertib and OAT family members.

The clinical implication is that the ipatasertib-induced inhibitory effects on hOAT4 function and expression might lead to transporter-mediated drug-drug interactions. In patients treated with ipatasertib combined with drugs for non-cancer-related diseases, the down-regulated hOAT4 expression and activity via PKB inhibition could reduce the renal elimination of other drugs if they are hOAT4 substrates and excreted by the transporter. The reduced renal elimination would increase concentrations of those drugs in the kidney and the blood and alter their pharmacokinetic profiles, potentially increasing therapeutic effects or causing toxicity. There are other specific PKB/Akt inhibitors, such as afuresertib, being developed and investigated in clinical studies for various types of cancer (42,43). The regulatory effects of PKB-inhibiting drugs on OAT family members will be an excellent topic for our future studies.

SUMOylation has become an important post-translational modification in regulating proteins after their synthesis. Membrane proteins are reported to be regulated by their SUMOylation, including potassium channel K2P1 and type I transforming growth factor-β receptor (12,14). Our previous studies found that hOAT3, another member of the

OAT family, is subject to SUMO modification (18,44). Although hOAT3 and hOAT4 are both multi-specific transporters from the same family, they differ in various aspects, including substrate specificity, tissue localization, and regulations (2,3,9,11,32). These two transporters should be studied individually *in vitro* to elucidate their transport functions and regulations. Thus, in this study, we focused on the effect of IGF-1 on hOAT4 SUMOylation and the involvement of PKB signaling. Our results (Figure 6) showed that hOAT4 was a target for endogenous SUMO modifications by SUMO1/2/3. However, IGF-1 can only upregulate hOAT4 conjugated to SUMO2 and SUMO3, and SUMO2 conjugation showed a higher degree of increase (Figure 7). Moreover, this increase induced by IGF-1 was reversed by the PKB-specific inhibitor ipatasertib (Figure 8), suggesting PKB played a central role in the IGF-1-mediated regulation of hOAT4 SUMOylation. This finding is consistent with the roles of PKB on hOAT4 expression and activity (Figures 3 & 4). Notably, IGF-1 upregulated the hOAT4 SUMOylation by SUMO2 and SUMO3, while the modification by SUMO1 was not significantly altered by IGF-1 (Figures 6 & 7). The heterogeneity between SUMO1 and SUMO2/3 comes in multiple aspects. Some of the SUMOylated proteins are modified exclusively by SUMO1 *in vivo*. And other target proteins can be conjugated to SUMO2/3 or all SUMO isoforms. In cells, SUMO2/3 proteins are usually more abundant than SUMO1, and the non-conjugated SUMO2/3 will be attached to target proteins promptly upon cellular stresses (12,16). Protein SUMOylation is a critical part for cellular responses to external stress, such as DNA damage, heat shock, and oxidative stress (45,46). During these responses, SUMO1 and SUMO2/3 often display different dynamics and functions. For example, SUMO1 shows a distinct distribution pattern and has slower dynamics than SUMO2 or SUMO3 (47). The dynamical transition of SUMO1 between SUMOylation and deSUMOylation is slower than that of SUMO2 and SUMO3 (12,14). Thereby, the individual roles of SUMO1/2/3 in hOAT4 SUMOylation might be different and will need further investigation in the future.

The majority of protein SUMOylation occurs around a consensus motif, Ψ-K-X-D/E (Ψ is a hydrophobic amino acid, K is the lysine residue for SUMOylation, X is any amino acid, D is an aspartic acid, and E is a glutamic acid) (12,48). We predicted potential SUMOylation sites of hOAT4 using an online tool called SUMOplot (Abcepta, San Diego, CA). The tool predicted that K131, K288, and K321 of hOAT4 could be SUMOylation sites with high probability. However, matching the consensus motif does not guarantee that a SUMO modification will occur at that site. Some SUMOylation sites are actually outside the consensus motif (12,13,48). Therefore, the SUMOylation sites of hOAT4 need to be confirmed in direct experimental approaches such as site-directed mutagenesis and mass spectrometry analysis.

Remote sensing and signaling is a theory describing communications across multiple tissues and organs to maintain overall homeostasis. The remote regulations of transporters are one of the central interactions of this network. Signaling molecules such as hormones and metabolites are generated from one organ and arrive at distal tissues to modulate transporters there (19,20). IGF-1 is an excellent example of this type of remote regulation: it is a growth hormone synthesized and secreted by the hepatocytes in the liver. After entering blood circulation, IGF-1 is able to regulate multiple transporters in the kidney, such as epithelial sodium channel, urate transporter 1, and in the current study, hOAT4 (21,25). The

physiological implication is that there are hepatic communications with hOAT4 expressed in the kidney and placenta, potentially altering the disposition of numerous therapeutics, toxins, and metabolites. Moreover, our study also indicated that this remote regulation of hOAT4 is mediated at the level of PKB signaling.

In conclusion, our study demonstrates that the hepatic hormone IGF-1 regulates the transport activity, expression, and SUMOylation of hOAT4 through PKB signaling. Our findings are consistent with the remote sensing and signaling theory, where OATs play an essential role in the remote communications among tissues. This regulation of hOAT4 discovered in the current study is mediated by IGF-1 and intracellular PKB signaling (Figure 10).

## Acknowledgements

This work was supported by grants (to Dr. Guofeng You) from the National Institute of General Medical Sciences (R01-GM079123 and R01-GM097000).

## Abbreviations:

| | |
|---|---|
| **hOAT4** | human organic anion transporter 4 |
| **IGF-1** | insulin-like growth factor 1 |
| **PKB** | protein kinase B |
| **PTM** | post-translational modification |
| **SUMO** | small ubiquitin-like modifier |
| **ES** | estrone sulfate |
| **Ipa** | ipatasertib |
| **IP** | immunoprecipitation |
| **IB** | immunoblotting |

## Reference

1. Takeda M, Babu E, Narikawa S, Endou H. Interaction of human organic anion transporters with various cephalosporin antibiotics. European Journal of Pharmacology. 2002 Mar;438(3):137–42. [PubMed: 11909604]
2. Zhou F, Hong M, You G. Regulation of human organic anion transporter 4 by progesterone and protein kinase C in human placental BeWo cells. American Journal of Physiology-Endocrinology and Metabolism. 2007 Jul;293(1):E57–61. [PubMed: 17341544]
3. Zhang J, Wang H, Fan Y, Yu Z, You G. Regulation of organic anion transporters: Role in physiology, pathophysiology, and drug elimination. Pharmacology & Therapeutics. 2021 Jan;217:107647. [PubMed: 32758646]
4. Hagos Y, Stein D, Ugele B, Burckhardt G, Bahn A. Human Renal Organic Anion Transporter 4 Operates as an Asymmetric Urate Transporter. JASN. 2007 Feb;18(2):430–9. [PubMed: 17229912]
5. Duan P, Li S, You G. Regulation of human organic anion transporter 4 by parathyroid hormone-related protein and protein kinase A. Int J Biochem Mol Biol. 2012;3(3):322–7. [PubMed: 23097748]

6. Liu C, Zhang J, You G. Interaction of Anticancer Drugs with Human Organic Anion Transporter hOAT4. Journal of Oncology. 2019 Feb 28;2019:1–8.
7. Kummu M, Sieppi E, Koponen J, Laatio L, Vähäkangas K, Kiviranta H, et al. Organic anion transporter 4 (OAT 4) modifies placental transfer of perfluorinated alkyl acids PFOS and PFOA in human placental ex vivo perfusion system. Placenta. 2015 Oct;36(10):1185–91. [PubMed: 26303760]
8. Lu Y, Meng L, Ma D, Cao H, Liang Y, Liu H, et al. The occurrence of PFAS in human placenta and their binding abilities to human serum albumin and organic anion transporter 4. Environmental Pollution. 2021 Mar;273:116460. [PubMed: 33485002]
9. Xu D, You G. Loops and layers of post-translational modifications of drug transporters. Advanced Drug Delivery Reviews. 2017 Jul;116:37–44. [PubMed: 27174152]
10. Yu Z, Liu C, Zhang J, Liang Z, You G. Protein kinase C regulates organic anion transporter 1 through phosphorylating ubiquitin ligase Nedd4-2. BMC Mol and Cell Biol. 2021 Dec;22(1):53. [PubMed: 34663225]
11. Czuba LC, Hillgren KM, Swaan PW. Post-translational modifications of transporters. Pharmacology & Therapeutics. 2018 Dec;192:88–99. [PubMed: 29966598]
12. Yang Y, He Y, Wang X, liang Z, He G, Zhang P, et al. Protein SUMOylation modification and its associations with disease. Open Biol. 2017 Oct;7(10):170167. [PubMed: 29021212]
13. Chang HM, Yeh ETH. SUMO: From Bench to Bedside. Physiological Reviews. 2020 Oct 1;100(4):1599–619. [PubMed: 32666886]
14. Ulrich HD. The Fast-Growing Business of SUMO Chains. Molecular Cell. 2008 Nov;32(3):301–5. [PubMed: 18995828]
15. Cartier E, Garcia-Olivares J, Janezic E, Viana J, Moore M, Lin ML, et al. The SUMO-Conjugase Ubc9 Prevents the Degradation of the Dopamine Transporter, Enhancing Its Cell Surface Level and Dopamine Uptake. Front Cell Neurosci. 2019 Feb 8;13:35. [PubMed: 30828290]
16. Saitoh H, Hinchey J. Functional Heterogeneity of Small Ubiquitin-related Protein Modifiers SUMO-1 versus SUMO-2/3. Journal of Biological Chemistry. 2000 Mar;275(9):6252–8. [PubMed: 10692421]
17. Wang H, Zhang J, You G. Activation of Protein Kinase A Stimulates SUMOylation, Expression, and Transport Activity of Organic Anion Transporter 3. AAPS J. 2019 Mar;21(2):30. [PubMed: 30761470]
18. Zhang J, You G. Peptide Hormone Insulin Regulates Function, Expression, and SUMOylation of Organic Anion Transporter 3. AAPS J. 2021 Mar;23(2):41. [PubMed: 33709304]
19. Nigam SK, Bush KT, Martovetsky G, Ahn SY, Liu HC, Richard E, et al. The Organic Anion Transporter (OAT) Family: A Systems Biology Perspective. Physiological Reviews. 2015 Jan;95(1):83–123. [PubMed: 25540139]
20. Rosenthal SB, Bush KT, Nigam SK. A Network of SLC and ABC Transporter and DME Genes Involved in Remote Sensing and Signaling in the Gut-Liver-Kidney Axis. Sci Rep. 2019 Dec;9(1):11879. [PubMed: 31417100]
21. Yakar S, Adamo ML. Insulin-Like Growth Factor 1 Physiology. Endocrinology and Metabolism Clinics of North America. 2012 Jun;41(2):231–47. [PubMed: 22682628]
22. Bach LA, Hale LJ. Insulin-like Growth Factors and Kidney Disease. American Journal of Kidney Diseases. 2015 Feb;65(2):327–36. [PubMed: 25151409]
23. Janecka A, Kołodziej-Rzepa M, Biesaga B. Clinical and Molecular Features of Laron Syndrome, A Genetic Disorder Protecting from Cancer. In Vivo. 2016 Aug;30(4):375–81. [PubMed: 27381597]
24. Kamenický P, Mazziotti G, Lombès M, Giustina A, Chanson P. Growth Hormone, Insulin-Like Growth Factor-1, and the Kidney: Pathophysiological and Clinical Implications. Endocrine Reviews. 2014 Apr 1;35(2):234–81. [PubMed: 24423979]
25. Hakuno F, Takahashi SI. 40 YEARS OF IGF1: IGF1 receptor signaling pathways. Journal of Molecular Endocrinology. 2018 Jul;61(1):T69–86. [PubMed: 29535161]
26. Cheng CW, Adams GB, Perin L, Wei M, Zhou X, Lam BS, et al. Prolonged Fasting Reduces IGF-1/PKA to Promote Hematopoietic-Stem-Cell-Based Regeneration and Reverse Immunosuppression. Cell Stem Cell. 2014 Jun;14(6):810–23. [PubMed: 24905167]

27. Hemmings BA, Restuccia DF. PI3K-PKB/Akt pathway. Cold Spring Harb Perspect Biol. 2012 Sep 1;4(9):a011189. [PubMed: 22952397]
28. Blake JF, Xu R, Bencsik JR, Xiao D, Kallan NC, Schlachter S, et al. Discovery and Preclinical Pharmacology of a Selective ATP-Competitive Akt Inhibitor (GDC-0068) for the Treatment of Human Tumors. J Med Chem. 2012 Sep 27;55(18):8110–27. [PubMed: 22934575]
29. Massacesi C, Di Tomaso E, Urban P, Germa C, Quadt C, Trandafir L, et al. PI3K inhibitors as new cancer therapeutics: implications for clinical trial design. Onco Targets Ther. 2016;9:203–10. [PubMed: 26793003]
30. Fan Y, Wang H, Yu Z, Liang Z, Li Y, You G. Inhibition of proteasome, but not lysosome, upregulates organic anion transporter 3 in vitro and in vivo. Biochemical Pharmacology. 2023 Feb;208:115387. [PubMed: 36549459]
31. Fan Y, You G. Proteasome Inhibitors Bortezomib and Carfilzomib Stimulate the Transport Activity of Human Organic Anion Transporter 1. Mol Pharmacol. 2020 Jun 1;97(6):384–91. [PubMed: 32234809]
32. Huo X, Liu K. Renal organic anion transporters in drug–drug interactions and diseases. European Journal of Pharmaceutical Sciences. 2018 Jan;112:8–19. [PubMed: 29109021]
33. Bhardwaj RK, Herrera-Ruiz D, Eltoukhy N, Saad M, Knipp GT. The functional evaluation of human peptide/histidine transporter 1 (hPHT1) in transiently transfected COS-7 cells. European Journal of Pharmaceutical Sciences. 2006 Apr;27(5):533–42. [PubMed: 16289537]
34. Chioukh R, Noel-Hudson MS, Ribes S, Fournier N, Becquemont L, Verstuyft C. Proton Pump Inhibitors Inhibit Methotrexate Transport by Renal Basolateral Organic Anion Transporter hOAT3. Drug Metab Dispos. 2014 Dec;42(12):2041–8. [PubMed: 25239859]
35. Nabekura T, Kawasaki T, Kamiya Y, Uwai Y. Effects of Antiviral Drugs on Organic Anion Transport in Human Placental BeWo Cells. Antimicrob Agents Chemother. 2015 Dec;59(12):7666–70. [PubMed: 26416870]
36. Zhang J, Yu Z, You G. Insulin-like growth factor 1 modulates the phosphorylation, expression, and activity of organic anion transporter 3 through protein kinase A signaling pathway. Acta Pharmaceutica Sinica B. 2020 Jan;10(1):186–94. [PubMed: 31993315]
37. Chenal J, Pierre K, Pellerin L. Insulin and IGF-1 enhance the expression of the neuronal monocarboxylate transporter MCT2 by translational activation via stimulation of the phosphoinositide 3-kinase-Akt-mammalian target of rapamycin pathway: MCT2 translational activation by insulin and IGF-1. European Journal of Neuroscience. 2007 Dec 17;27(1):53–65. [PubMed: 18093179]
38. Zhu H, Xu Y, Gong F, Shan G, Yang H, Xu K, et al. Reference ranges for serum insulin-like growth factor I (IGF-I) in healthy Chinese adults. PLoS One. 2017;12(10):e0185561. [PubMed: 28976993]
39. Buckingham L, Hao T, O'Donnell J, Zhao Z, Zhang X, Fan Y, et al. Ipatasertib, an oral AKT inhibitor, inhibits cell proliferation and migration, and induces apoptosis in serous endometrial cancer. Am J Cancer Res. 2022;12(6):2850–62. [PubMed: 35812065]
40. Malhi V, Budha N, Sane R, Huang J, Liederer B, Meng R, et al. Single- and multiple-dose pharmacokinetics, potential for CYP3A inhibition, and food effect in patients with cancer and healthy subjects receiving ipatasertib. Cancer Chemother Pharmacol. 2021 Dec;88(6):921–30. [PubMed: 34471960]
41. Sweeney C, Bracarda S, Sternberg CN, Chi KN, Olmos D, Sandhu S, et al. Ipatasertib plus abiraterone and prednisolone in metastatic castration-resistant prostate cancer (IPATential150): a multicentre, randomised, double-blind, phase 3 trial. The Lancet. 2021 Jul;398(10295):131–42.
42. Spencer A, Yoon SS, Harrison SJ, Morris SR, Smith DA, Brigandi RA, et al. The novel AKT inhibitor afuresertib shows favorable safety, pharmacokinetics, and clinical activity in multiple myeloma. Blood. 2014 Oct 2;124(14):2190–5. [PubMed: 25075128]
43. Nitulescu GM, Margina D, Juzenas P, Peng Q, Olaru OT, Saloustros E, et al. Akt inhibitors in cancer treatment: The long journey from drug discovery to clinical use (Review). International Journal of Oncology. 2016 Mar;48(3):869–85. [PubMed: 26698230]

44. Yu Z, Zhang J, Liang Z, Wu J, Liu K, You G. Pancreatic Hormone Insulin Modulates Organic Anion Transporter 1 in the Kidney: Regulation via Remote Sensing and Signaling Network. AAPS J. 2023 Jan 10;25(1):13. [PubMed: 36627500]

45. Hickey CM, Wilson NR, Hochstrasser M. Function and regulation of SUMO proteases. Nat Rev Mol Cell Biol. 2012 Dec;13(12):755–66. [PubMed: 23175280]

46. Enserink JM. Sumo and the cellular stress response. Cell Division. 2015 Jun 20;10(1):4. [PubMed: 26101541]

47. Ayaydin F, Dasso M. Distinct In Vivo Dynamics of Vertebrate SUMO Paralogues. MBoC. 2004 Dec;15(12):5208–18. [PubMed: 15456902]

48. Matic I, Schimmel J, Hendriks IA, van Santen MA, van de Rijke F, van Dam H, et al. Site-Specific Identification of SUMO-2 Targets in Cells Reveals an Inverted SUMOylation Motif and a Hydrophobic Cluster SUMOylation Motif. Molecular Cell. 2010 Aug;39(4):641–52. [PubMed: 20797634]

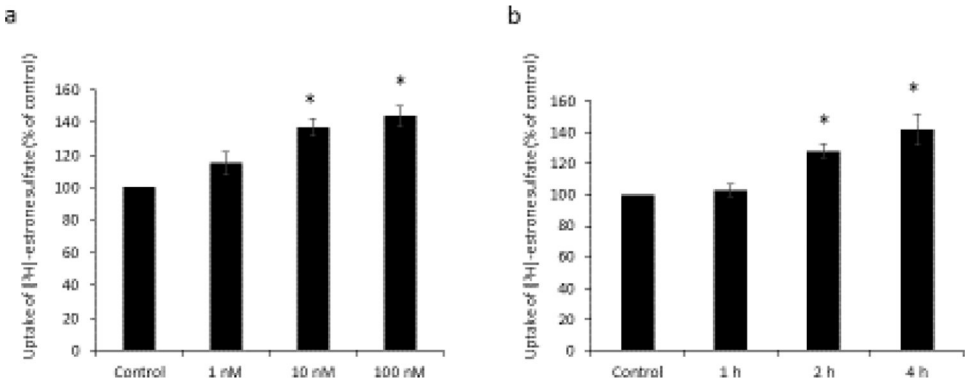


**Figure 1. Dose- and time-dependent effects of IGF-1 on hOAT4 transport activity in COS-7 cells.**

**(a)** hOAT4-expressing COS-7 cells were treated with various concentrations of IGF-1 for 2 h, followed by [$^3$H]-estrone sulfate (ES) uptake (4 min, 0.3 μM of ES). Uptake activity was expressed as a percentage of the uptake measured in control cells. The data represent uptake into hOAT4-expressing cells minus uptake into parental COS-7 cells and were normalized by total protein concentration from each group. Values are mean ± S.D. (n = 3). *P < 0.05. **(b)** hOAT4-expressing cells were treated with 100 nM IGF-1 for 1, 2, 4 hours, followed by [$^3$H]-ES uptake (4 min, 0.3 μM of ES). Uptake activity was expressed as a percentage of the uptake measured in control cells. The data represent uptake into hOAT4-expressing cells minus uptake into parental COS-7 cells and were normalized by total protein concentration from each group. Values are mean ± S.D. (n = 3). *P < 0.05.

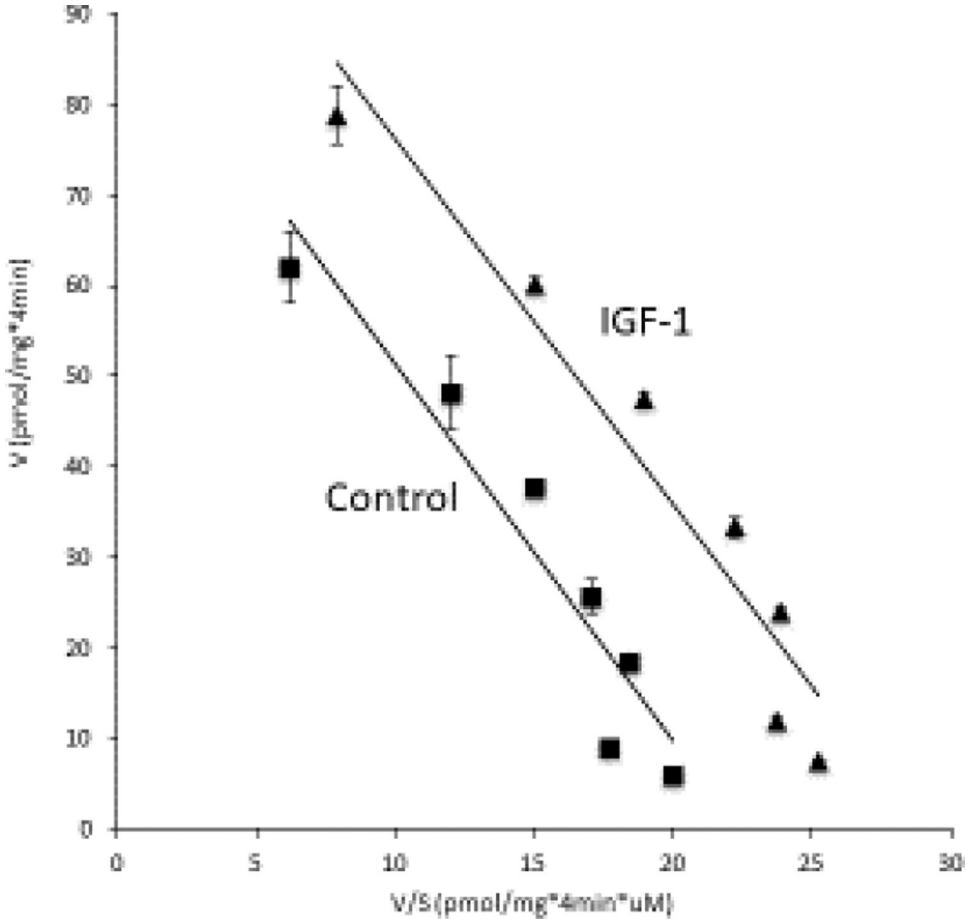


**Figure 2. Effect of IGF-1 on kinetics of hOAT4-mediated estrone sulfate transport.**

COS-7 cells expressing hOAT4 were treated with IGF-1 (100 nM, 2 h), and uptake of [$^3$H]-estrone sulfate (ES) was measured at a series of concentrations of 0.1 – 10 μM of ES. The data represent uptake into hOAT4-transfected cells minus uptake into parental COS-7 cells and were normalized by total protein concentration from each group. Transport kinetic values ($V_{max}$ and $K_m$) were calculated using the Eadie-Hofstee transformation. Values are means ± S.D. (n = 3). V, velocity; S, substrate concentration.

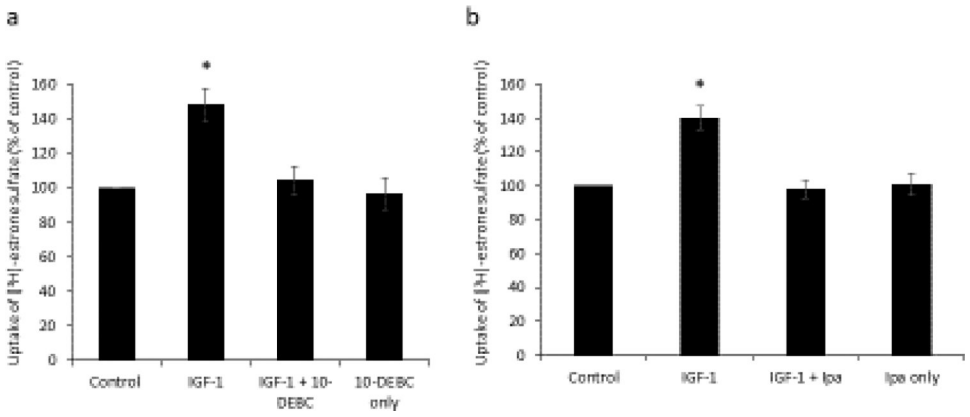


**Figure 3. PKB inhibitors blocked IGF-1-stimulated hOAT4 transport activity.**

**(a)** hOAT4-expressing cells were treated with 100 nM of IGF-1 for 2 h with or without 7 μM of 10-DEBC, a PKB-specific inhibitor. hOAT4-mediated uptake (4 min) of [$^3$H]-estrone sulfate (ES) was then measured. Uptake activity was expressed as a percentage of the uptake measured in control cells. The data represented uptake into hOAT4-expressing cells minus uptake into parental cells. Values are mean ± S.D. (n = 3). *$p < 0.05$. **(b)** hOAT4-expressing cells were treated with 100 nM of IGF-1 for 2 h with or without 10 μM of ipatasertib (Ipa), an anti-cancer drug specifically inhibiting PKB. hOAT4-mediated uptake (4 min) of [$^3$H]-ES was then measured. Uptake activity was expressed as a percentage of the uptake measured in control cells. The data represented uptake into hOAT4-expressing cells minus uptake into parental cells. Values are mean ± S.D. (n = 3). *$p < 0.05$.

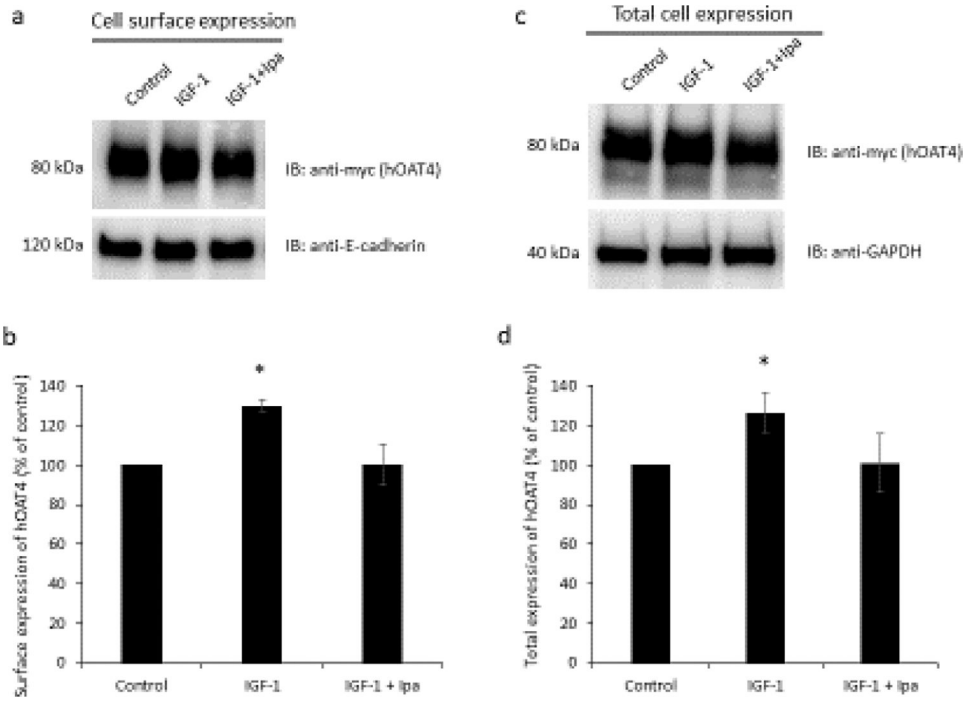


**Figure 4. Effects of IGF-1 and ipatasertib on hOAT4 protein expression.**

**(a)** Top panel: cell surface expression of hOAT4. hOAT4-expressing cells were treated with IGF-1 (100 nM, 2 h), with or without 10 μM ipatasertib (Ipa). Cells were then labeled with biotinylation reagent and lysed. Biotinylated proteins were purified with streptavidin beads, followed by immunoblotting (IB) with anti-myc antibody. Epitope myc was tagged to hOAT4 for immune-detection. Bottom panel: the same blot from top panel was stripped and reprobed with anti-E-cadherin antibody. E-cadherin is a cell membrane protein marker. **(b)** Densitometry plot of results from Figure 4a as well as from other experimental repeats. Density values have been normalized to loading control from the same blot. The values are mean ± S.D. (n = 3). *P < 0.05. **(c)** Top panel: cellular total expression of hOAT4. hOAT4-expressing cells were treated with IGF-1 (100 nM, 2 h), with or without 10 μM ipatasertib. Treated cells were lysed and followed by immunoblotting with anti-myc antibody. Bottom panel: the same blot from top panel was stripped and reprobed with anti-GAPDH antibody. GAPDH is a cellular protein marker. **(d)** Densitometry plot of results from Figure 4c as well as from other experimental repeats. Density values have been normalized to loading control from the same blot. The values are mean ± S.D. (n = 3). *P < 0.05.

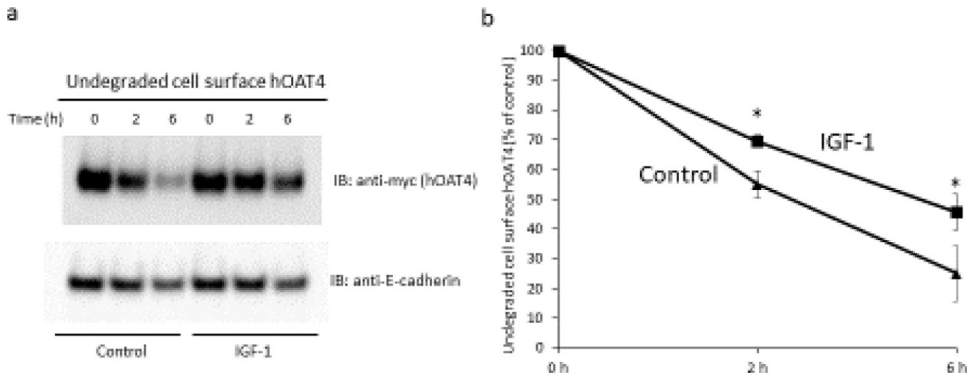


**Figure 5. IGF-1 reduced the degradation rate of cell surface hOAT4.**

**(a)** COS-7 cells expressing hOAT4 were biotinylated and then treated with 100 nM of IGF-1 for 2 or 6 hours under cell culture condition. The degradation of biotinylated cell surface hOAT4 was then determined as described in the “Materials and Methods” section. E-cadherin was measured on the same blot as a cell membrane protein marker. **(b)** Densitometry plot of results from Figure 5a as well as from other experimental repeats. The amount of undegraded cell surface hOAT4 was expressed as a percentage of the total amount of initial cell surface hOAT4. Density values have been normalized to loading controls from the same blot. Values are mean ± S.D. (n = 3). *P < 0.05.

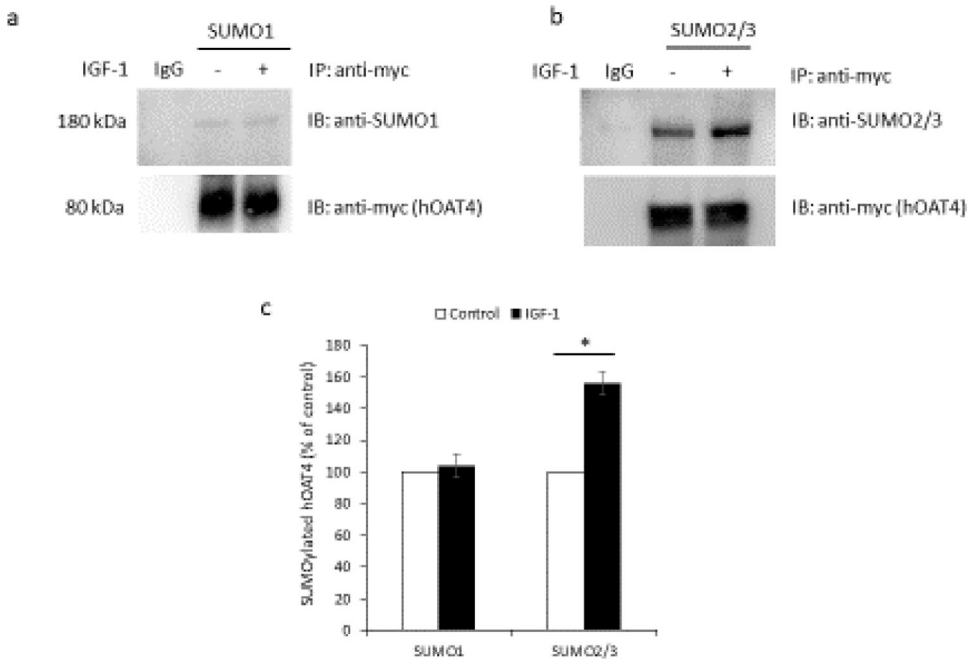


**Figure 6. The involvement of endogenous SUMO1/2/3 in hOAT4 SUMOylation.**

**(a)** Top Panel: hOAT4-expressing cells were treated with IGF-1 (100 nM, 2 h). Myc-tagged hOAT4 was then immunoprecipitated (IP) by anti-myc antibody, followed by immunoblotting (IB) with anti-SUMO1 antibody to detect hOAT4 SUMOylated by endogenous SUMO1. Bottom panel: The same blot from top panel was stripped and reprobed with anti-myc antibody to detect the total amount of pulled-down hOAT4. **(b)** Top Panel: hOAT4-expressing cells were treated with IGF-1 (100 nM, 2 h). hOAT4 was then immunoprecipitated (IP) by anti-myc antibody, followed by immunoblotting (IB) with anti-SUMO2/3 antibody to detect hOAT4 SUMOylated by endogenous SUMO2/3. Bottom panel: The same blot from top panel was stripped and reprobed with anti-myc antibody to detect the total amount of pulled-down hOAT4. **(c)** Densitometry plot of results from Figure 6a and 6b as well as from other experimental repeats. Density values have been normalized to total hOAT4 pulled-down from the same blot. Values are mean ± S.D. (n = 3). *P < 0.05.

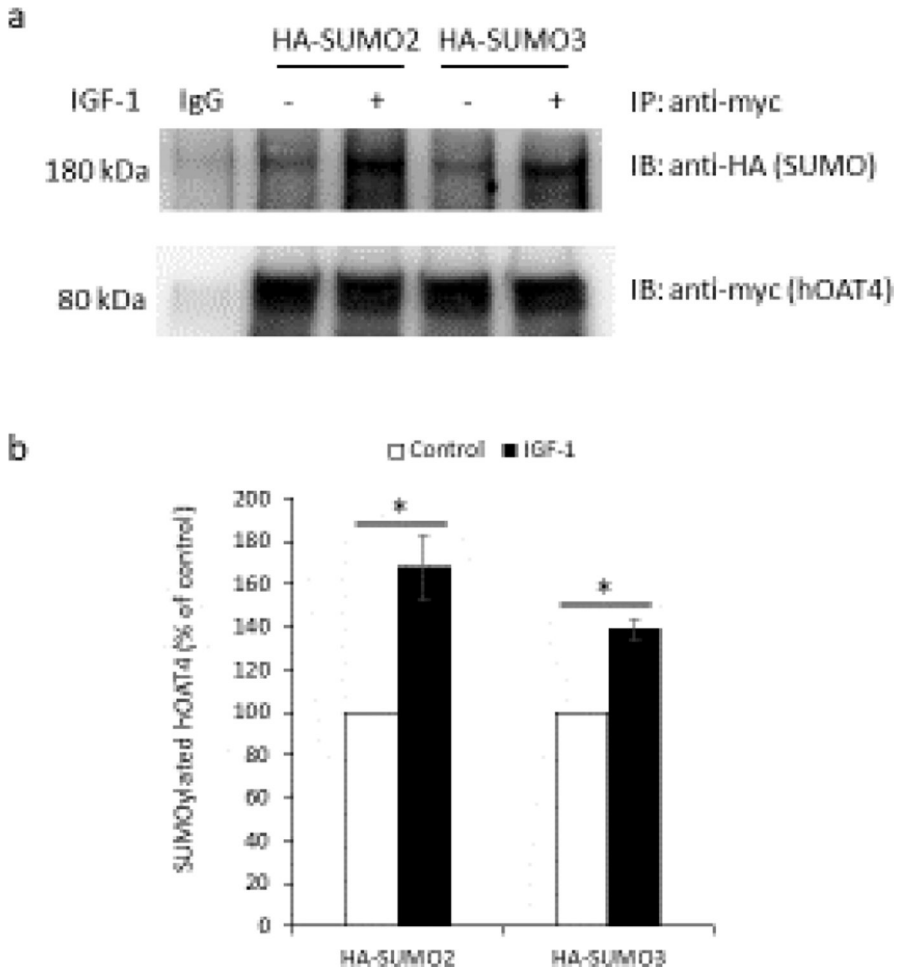


**Figure 7. The involvement of transfected SUMO2/3 in hOAT4 SUMOylation.**

**(a)** Top panel: hOAT4-expressing cells were individually transfected with HA-SUMO2 or HA-SUMO3 and treated with IGF-1 (100 nM, 2 h). Myc-tagged hOAT4 was immunoprecipitated (IP) by anti-myc antibody, followed by immunoblotting (IB) with anti-HA antibody to detect SUMOylated hOAT4. Bottom panel: the same blot from top panel was stripped and reprobed with anti-myc antibody to detect the total amount of pulled-down hOAT4. **(b)** Densitometry plot of results from Figure 7a as well as from other experimental repeats. Density values have been normalized to total hOAT4 pulled-down from the same blot. Values are mean ± S.D. ($n$ = 3). *P < 0.05.

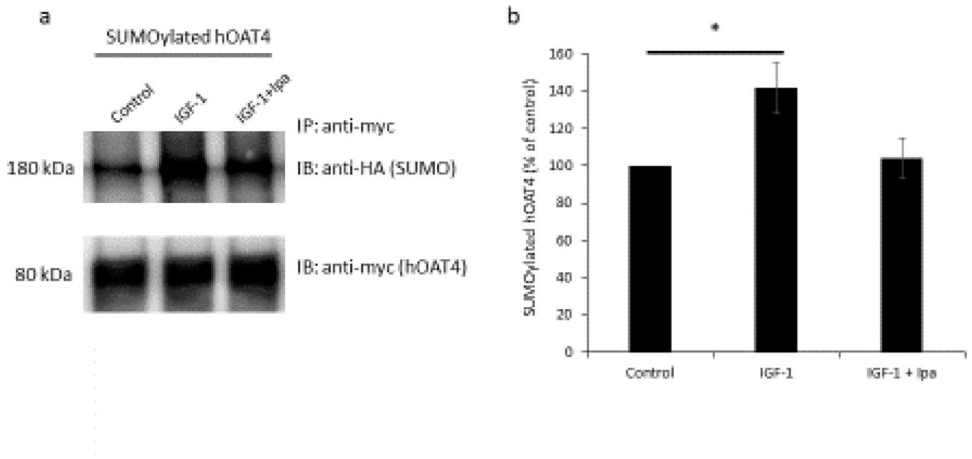


**Figure 8. Effects of IGF-1 and ipatasertib on hOAT4 SUMOylation.**

**(a)** Top panel: hOAT4-expressing cells were transfected with HA-SUMO2 and treated with IGF-1 (100 nM, 2 h) in the absence and presence of 10 μM ipatasertib (Ipa). Myc-tagged hOAT4 was immunoprecipitated (IP) by anti-myc antibody, followed by immunoblotting (IB) with anti-HA antibody to detect SUMOylated hOAT4. Bottom panel: the same blot from top panel was stripped and reprobed with anti-myc antibody to detect the total amount of pulled-down hOAT4. **(b)** Densitometry plot of results from Figure 8a as well as from other experimental repeats. Density values have been normalized to total hOAT4 pulled-down from the same blot. Values are mean ± S.D. ($n$ = 3). *P < 0.05.

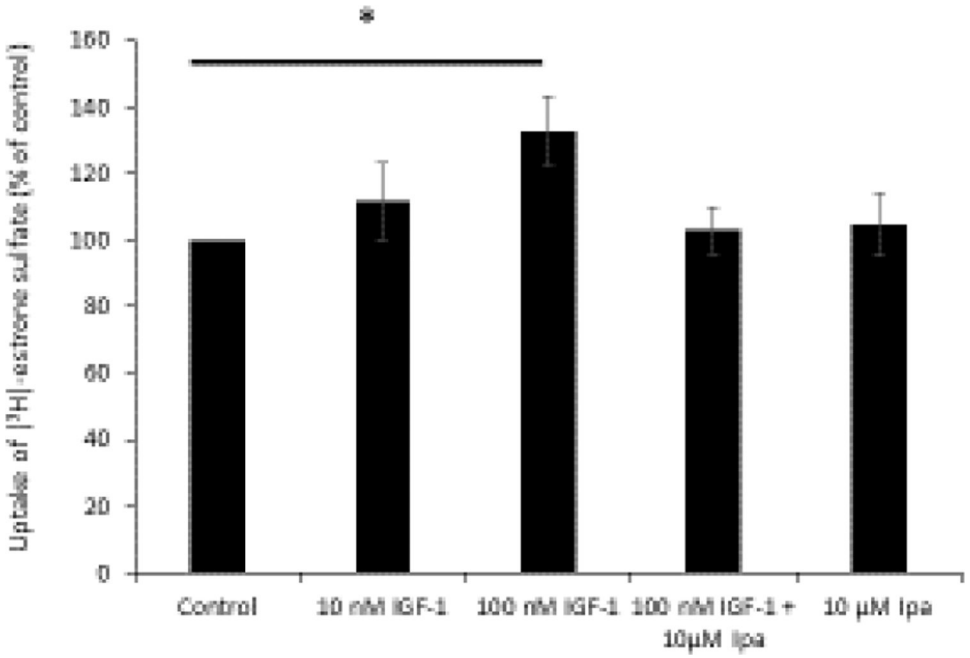


**Figure 9. Effects of IGF-1 and ipatasertib on hOAT4 transport activity in placental BeWo cells.**

hOAT4-expressing BeWo cells were treated with IGF-1 (10 – 100 nM, 4 h) with or without 10 μM ipatasertib (Ipa), followed by [$^3$H]-ES uptake (4 min, 0.3 μM of ES). Uptake activity was expressed as a percentage of the uptake measured in control cells. The data represent uptake into hOAT4-expressing BeWo cells minus uptake into parental BeWo cells and were normalized to total protein concentration from each group. Values are mean ± S.D. (n = 3). *P < 0.05.

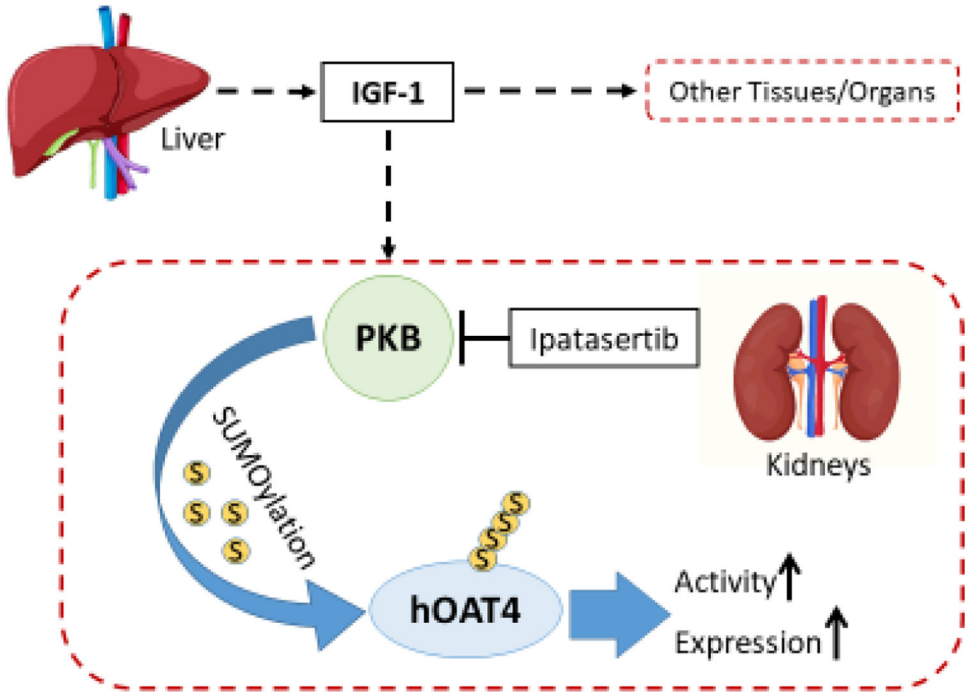


**Figure 10.**
IGF-1 regulates hOAT4 via the remote sensing and signaling network.